Planar chip device for PCR and hybridization with surface acoustic wave pump

Zeno Guttenberg,*[a] Helena Müller,[a] Heiko Habermüller,[a] Andreas Geisbauer,[a] Jürgen Pipper,[b] Jana Felbel,[b] Mark Kielpinski,[b] Jürgen Scriba[a] and Achim Wixforth[ac]

DOI: 10.1039/b412712a

We have developed a microfluidic device operating at a planar surface instead of a closed channel network. The fluid is transported in single droplets using surface acoustic waves (SAW) on a piezoelectric $LiNbO_3$ substrate. The surface of the piezo is chemically structured to induce high contact angles of the droplets or enclose areas where the liquid can wet the substrate. Combining the SAW technique with thin film resistance heaters, a biological analysis chip with integrated DNA amplification by PCR and hybridization was designed. To prevent evaporation of the PCR reagents at high temperatures the sample is enclosed in droplets of mineral oil. On this chip the SAW resolves dried primers, shifts the oil capped liquid between the two heaters and mixes during hybridization. The chip is able to perform a highly sensitive, fast and specific PCR with a volume as low as 200 nl. During the temperature cycles an online monitoring of the DNA concentration is feasible with an optical unit, providing a sensitivity of 0.1 ng. After PCR the product is moved to the second heater for the hybridization on a spotted DNA array. With our chip we were able to detect a single nucleotide polymorphism (SNP) responsible for the Leiden Factor V syndrome from human blood.

1. Introduction

Employing microfluidic systems, biological analysis assays can be reduced to a very small scale.[1–4] The transition from macroscopic sample handling to miniaturized chip based devices has several advantages: The reduced size allows for the integration of processes from sample preparation to analysis in a single lab-on-a-chip. As manual handling between single steps can be eliminated, the process speed is increased and the risk of contamination is minimized. Moreover, the small sample volumes help to reduce costs for reagents and enhance efficiency and sensitivity of the analysis. The compact PCR-labchip can easily be used in conjunction with pipetting robots for high-throughput automation and is also a key component of future cellphone-sized equipment for near-patient diagnostics.

Most microfluidic systems are constructed using closed channel networks fabricated in glass, silicon or plastic, in which the liquid is moved with external or integrated miniaturized pumps and valves. Another approach uses channels in soft polymer layers that can be pneumatically deformed to induce liquid motion or to lock up cavities.[5] With the reduction of the channel size additional physical effects can be utilized. The so-called electrokinetic or electrocapillary effects can be exploited to handle and control a fluid flow in diameters close to the screening length of the ions in solution.[6,7]

However, the concept of microfluidics as a closed system has to deal with some major problems. The pressure required to move the liquid scales inversely with the channel dimension.[8] This means, that the power of the pumps therefore has to be increased in the same way the size is reduced, which complicates an integration into a complete system. With hydrophilic channels that are filled by capillary forces no pumps are needed, but the fluid control is delicate. Furthermore, when a biological solution is pumped through a narrow tube, the risk of reagent loss by adhesion to the wall is large due to the unfavourable surface to volume ratio. Other problems are that small channels can easily get clogged and that surface modification and functionalization is difficult to control.

To process small volumes in a short amount of time was one of the motivations for the development of on-chip PCR.[9–21] Successful PCR was shown for volumes of one microliter down to even one picoliter.[22] In a $V = 1.7$ µl chamber sufficient amplification could be managed in 15 cycles in about 4 min[23] and another group reached 30 s for one cycle with $V = 280$ nl.[24] The aspect of sensitivity was much less addressed in the investigation of microfluidic PCR devices. Starting concentrations normally were in the upper nanogram range. Only a few researchers investigated the amplification of a low amount of template DNA. The highest sensitivity that can be reached with a PCR device is the successful amplification of a single DNA template. This was shown by Lagally *et al.* for a glass microchamber.[24,25]

Here, we would like to present a completely different approach to liquid handling on small scales, that instead of closed tubing uses a chemically modified surface to provide virtual fluid confinement. The distribution of the fluid on the surface is controlled by the surface free energy and not by channel walls. Depending on the kind of chemical modification droplets with high contact angle will form (hydrophobic) or the liquid will wet the surface (hydrophilic). On a chemically

*guttenberg@advalytix.de

heterogeneous surface produced in a structuring process, a fluid can be exactly confined inside a hydrophilic region surrounded by a hydrophobic area. The chemical modification can be achieved by coating with silanes[26] or thiols[27,28] depending on the kind of substrate used. To structure the resulting organic films, photolithography or micro-contact printing[29] are the easiest to apply.

On a hydrophobic surface a microliter amount of aqueous liquid will form a droplet, a closed compartment, having the shape of a sphere and a small interface to the solid. Therefore different reagent solutions can be placed on the surface of the same chip without getting in touch with each other. In a channel system valves or a separation medium would be needed for the same task. For a microfluidic device, it is necessary to move the droplets to bring reagents into contact. For the actuation of liquids on a solid surface different approaches have been published. Electrowetting describes the effect of changing the surface tension of a fluid with an electric potential induced by two electrodes.[30] To move a droplet, an array of electrode pairs is fabricated with a voltage applied successively to the single pairs. The electrodes are normally situated on two opposite plates that are separated by air or an immiscible fluid.[31,32] Another possibility is to use the chemical modification of the substrate itself for the actuation. On a gradient of the surface free energy[33,34] a small amount of liquid will move in the direction of increasing hydrophilicity. Other groups report using light sensitive materials that change their surface energy during illumination.[35] Furthermore, a soluble hydrophilic layer on a hydrophobic solid induces a constant fluid motion until the whole layer is dissolved.[36] Lyuksyutov *et al.*[37] even managed to agitate isolated femtoliter droplets close to a surface *via* diamagnetic levitation.

Our approach is to use surface acoustic waves (SAW) on a piezoelectric substrate for the droplet actuation.[38,39] The waves are generated by interdigitated gold electrodes (IDT) being connected to a high frequency (RF) power source. The fast alternating electric field generates displacements on the surface of the piezo with an amplitude in the nm range, moving at speed of sound on the substrate. When a fluid is placed in the propagation path of the SAW a momentum is transferred to it. Small droplets are actuated in the same direction as the wave when sufficient RF power is applied. As described in a previous paper the SAW in contact with liquid can also be used for mixing[40] and for dispensing small droplets out of a larger volume.[41] The latter results were obtained on a chemically structured surface.

The SAW is generated by an IDT structure that is patterned with the help of photolithography on a planar $LiNbO_3$ substrate. With the same process other metal structures can be established as well. This allows one to build up a chip with different functional units. The transport of liquid between the units can be achieved by the SAW. The chemical patterning also helps to dispense and guide droplets. The first functional structure we tested on the chips is a metal thin film resistance heater with an integrated temperature sensor. The heater is 2×2 mm^2 in size and has an window in the middle, allowing for optical observation through the transparent piezoelectric substrate. The temperature is computer controlled with 0.1 K accuracy.

A chip heater can be used for two processes in DNA analysis. The first is the amplification of a small amount of template DNA called polymerase chain reaction (PCR)[42] where repeated cycles of three different temperatures lead to amplification of the DNA strands. To analyze the amplified DNA, hybridization assays are commonly used.[43] Employing this method the binding of DNA in solution to surface coupled complementary strands is observed, while the temperature is kept on a value characteristic for the reactants. This provides information on the corresponding nucleotide sequence. With the two processes performed subsequently on one chip, a tool for complete DNA analysis is built suitable for various applications like the study of gene function, gene expression and single nucleotide polymorphism (SNP).[44,45]

To prevent evaporation of the reagents on the open surface of our chip, the aqueous solution is covered with mineral oil, that forms a circular shaped cap due to the chemical modification of the surface. The application of the oil cap can be also achieved with the help of the SAW actuation, by simply pushing the oil onto the water droplet, while the different surface tensions of the two liquids account for the spatial arrangement. Therefore encapsulation of the PCR solution against evaporation can be reached much simpler than with valves in a microfluidic channel system. The contact area of the oil/water droplet to the chip plane has about the size of the heater structure. This whole fluid "microchamber" can also be moved on the chip with the SAW. The speed, volume and sensitivity of PCR on a planar chip has been compared to that in closed channel devices in separate experiments.[46,47]

To gain better control over progress and efficiency of the PCR, an optical online monitoring system was integrated. This can be done with different fluorescent dye systems, that exhibit varying emission intensities correlated with the amount of double stranded DNA or the concentration of a special DNA product with their emission intensity.[48] Several devices are already commercially available for online detection of PCR products and different groups showed successful monitoring[12,49] for their microfluidic devices. To investigate the possibilities for a direct PCR process control on our planar chip we designed a small optical unit that can collect the light emitted from a dye inside the oil covered PCR droplet. The unit is placed below the transparent chip and the optical path is focused through the window in the heater structure into the aqueous solution. This yields information on the amount of amplified DNA and helps to optimize the cycle parameters.

Our chip comprises two heater structures, one of which is used for PCR while the other can be used for hybridization of the PCR product. In the hybridization process, labeled mobile DNA molecules bind to complementary strands being linked to a solid surface. The covalent coupling requires a specific surface chemistry, usually epoxy groups. A square 1×1 mm^2 array of this chemical modification was applied to the chip in the center of the second heater with a patterning process. Since a surface modified with epoxy groups is hydrophilic, the PCR solution can wet it during hybridization. Furthermore, epoxy modified lines are also used to guide the movement of droplets on the chip actuated by SAW. Hence, the array and the tracks

can be generated in the same photolithographic structuring, while the rest of the chip is kept hydrophobic.

After the last PCR cycle the oil/water droplet is moved to the epoxy array with the SAW. When the two aqueous bubbles of equal volume get in close contact, they get united inside the oil. After mixing with the SAW the hybridization temperature is set. The detection of the fluorescence of the processed hybridization array is done with a commercial slide scanner.

In this paper we demonstrate the successful detection of a SNP with our planar chip and therefore show the possibility to built up a lab-on-a-chip device on a SAW chip with integrated thin film heaters. We hope to convince the reader that the planar SAW chip with a non-contact acoustic nanopump can be a simple and cheap alternative for the design of biological diagnostic devices.

2. Experimental

2.1 Droplet agitation with SAW

We first want to give a short overview over the technique of SAW driven droplet movement on the surface of a $LiNbO_3$ chip. An example for a microfluidic processor designed to position and move reagents will be shown.

Agitation of small droplets on the surface of a SAW chip is caused by the effect of acoustic streaming. This phenomenon appears when intensive sound fields are traveling through a liquid. The amplitude of the sound is attenuated by the viscosity of the medium during its propagation. This leads to a pressure gradient in the liquid. If the gradient is large, the fluid starts to move in the same direction as the sound wave.[50,40]

The SAW can also induce intensive sound fields in liquids. When it reaches the contact line of a droplet on the chip surface it gets strongly absorbed by the liquid. This leads to a fast decay of the amplitude and an excitation of a sound wave. With the sufficient RF power applied to induce the SAW, the generated sound wave leads to acoustic streaming that circulates the fluid inside the droplet. This motion can be used to mix or dissolve reagents.

When the RF power is increased, the whole droplet starts to move across the surface in the direction of the SAW. The RF power threshold for the movement strongly depends on the contact angle of the droplets. On hydrophilic substrates, the value of the threshold is notedly higher. Beyond the threshold increasing the RF power leads to higher speed of the droplets. Velocities larger than 5 cm s^{-1} can be reached.

Actuation with SAW can be applied from few picoliters up to several microliters. The droplets on the surface of a SAW chip can be moved along the propagation paths of the acoustic wave having the same width as the IDTs. The SAW can be induced in two perpendicular directions on the piezo substrate. This means that a droplet that reaches the crossing of two propagation paths is forced into a 90° turn (Fig. 1). So with a proper arrangement of IDTs most of the area of a chip is accessible with the SAW actuation.

The amplitude of the SAW decreases rapidly when it reaches the contact line of the liquid and is attenuated by orders of magnitude after several wavelengths. This means that when two droplets are successively placed in an acoustic path only the one closer to the IDT will be moved. They can therefore be merged with two opposing IDTs (Fig. 1).

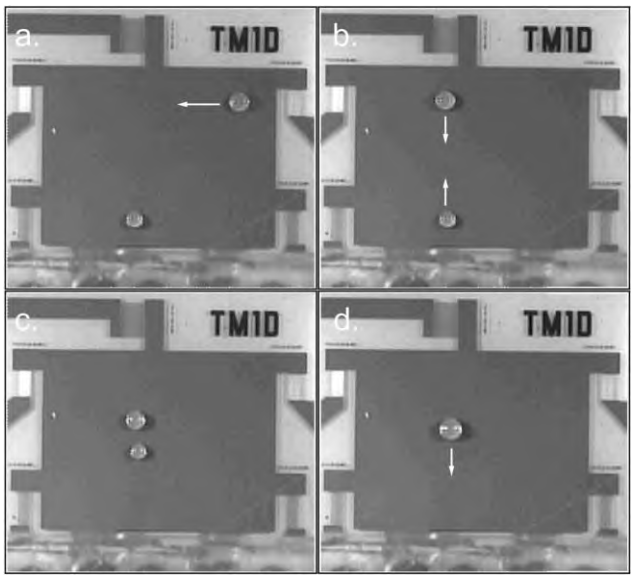

Fig. 1 Droplet movement with SAW on a microfluidic processor chip with 6 IDTs. The surface of the chip was made hydrophobic by an organic silane layer. The setup is cooled to prevent evaporation of the liquid. (a): Droplet is actuated from the right upper IDT to the crossing with the perpendicular acoustic path. (b): Both droplets are moved by the perpendicular transducers. (c): Both droplets shortly before merging. (d): Droplets have merged and can be further moved to a different position on the chip. The volume of the droplets is $V = 200$–300 nl.

2.2 Design and fabrication of the PCR-Chip

The base material of the chips is a 128° rotated Y-cut $LiNbO_3$ single crystal wafer polished on both sides. The first metal layer is Pt or Ni for the heater and sensor structure, followed by a gold layer for the SAW transducer and the contact wires. The complete chip is protected with sputtered silicon dioxide, which is removed above the contact pads. All structures are patterned by photolithography.

Each chip (Fig. 2.) has two heaters with a 1 × 1 mm window in the middle, surrounded by the temperature sensor. The sensors of the chips are calibrated by a thermoplate and resistance measurements controlled by a *LabView* program. The resistance was measured for five different temperatures in the range from 50 to 95 °C. The resistance *vs.* temperature data for the Pt wires show a linear dependence, for Ni sensors a second order term is needed to fit the data.

The chips have eight separately addressable SAW transducers, two on each side for aligning the droplets on the heater structures and for mixing during hybridization. Opposing transducers have different spatial periods to avoid crosstalk. The RF frequencies of the transducers are close to 150 MHz.

To form a high contact angle of the oil on the chips, the surface has to be lipophobic. However, the hybridization array has to be wetted easily and needs active coupling groups for the oligo DNA spots. Therefore a chemically heterogeneous

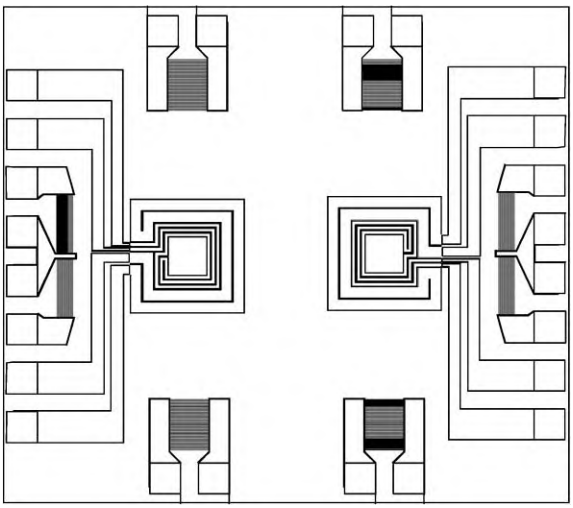

Fig. 2 SAW chip with eight interdigital transducers (black rectangles) and two thin film heaters with a 1 × 1 mm^2 window in the center. The windows are surrounded by the temperature sensors, followed by the heater wires. The whole chip is 15 × 13 mm^2.

surface modification is needed. This is achieved by photolithography. A 1 × 1 mm^2 square for the array and guiding tracks for the oil droplet movement are patterned on the chip with positive photo resist. An organic layer of a hydrophobic perfluoroalkylsilane is bound to the whole surface. After removing the photoresist, epoxysilane is grafted from an organic solution. Finally the chip is stored under argon atmosphere.

2.3 Instrumentation

The setup for the online PCR-chip with integrated hybridization consists of the following components: online detection with chip holder, heater control, RF-unit and control software. For the detection we use a small epi-illumination fluorescence microscope built from standard optical parts (*Owis*). Using this microscope, the progress of the PCR can be monitored through the detection window within the heater structure. Fluorescence of SYBR Green (*Roche*) intercalating dye emitted from the PCR sample drop is excited by a blue LED array and detected by either a photodiode detector or a CCD camera. Electrical and RF contact to the chip is achieved using a clamping mechanism holding contact pins.

The resistance of the sensor structure on the chip is determined by a 4 point measurement. Using a calibration curve for the particular chip the resistance is converted into temperature readings. A digital feedback (PID) algorithm was programmed to a microcontroller to regulate the voltage supply of the heater. Both the acquisition of the fluorescence intensity signal and the PCR cycle control are managed by the same *JAVA* based software.

In our prototype setup, a joystick controlled radio frequency generator is used to activate the SAW transducers on the chip. Using this joystick, droplets can be actuated in a very precise manner in either direction. Of course, this actuation can also be programmed and then computer controlled.

2.3 PCR and hybridization

The templates used for the experiments were the pGEM-Zf(+) plasmid from *Promega* and genomic DNA. Out of the first a 260 bp and from the second a 1382 bp and a 150 bp DNA fragment were amplified. Each PCR sample was covered by 5 µl of mineral oil. The primers for the plasmid were designed with the program *Primer3* (CCGGAAGCATAAAGTGTAAAGC and GTATTACCGCCTTTGAGTGAGC). The long genomic DNA fragment was amplified with the hu M1-1 and hu M1-2 primers for the muscarinic receptor (CCTAGCCACCATGAACACTTCAGC and GTAGGGAGCGGACGATGCTAGCTGG). For the short fragment the primer pair CTGTACTCAACTTAAGTTGTTCT and CTTAGTAAATATTTCTAATGGGG was used.

Three different kinds of experiments were performed on the chips: (1) PCR followed by gel electrophoresis: A kit from *Quiagen* was mixed with a 1 µM solution of the primers and different amounts of template DNA. Volumes in the range between 1 µl and 250 nl were pipetted onto one of the heaters and covered with oil to prevent evaporation. After cycling the whole droplet was removed from the chip and mixed with the gel loading buffer in a small PCR tube. The aqueous phase was extracted from the oil and loaded on a 8% polyacrylamid gel. The gel run was performed in a *Sigma* electrophoresis chamber. To reach a high sensitivity the DNA bands were visualized with the silver staining method. (2) PCR with online detection: The water/oil droplet was arranged in the same way to one of the heater windows as in the former experiments but with the SYBR green PCR kit from *Roche* added. The focus of the optical unit is set to the middle of the PCR droplet with the help of the CCD camera. During the heat cycles the actual state of the amplification is monitored by the control software. (3) PCR followed by hybridization. An 2 × 2 array of oligonucleotides was printed with a *Gene machines* spotter in the 1 × 1 mm^2 epoxy array in the left heater window. The spotting buffer was 5 × SSPE (saline-sodium phosphate EDTA, *Sigma*) and the size of the spots was 130 µm in diameter. After 12 h at 42 °C the chips were washed with a 0.2% SDS solution and incubated in 50 °C water for 20 min. To create a complete analysis chip with all the necessary probes on it, 0.5 µl of a 50 nM solution of the two primers was pipetted into the right heater window and incubated at room temperature until the water was evaporated. One of the primers was labeled with the dye Cy3. For long time storage the chips were kept under argon atmosphere.

Before the experiment 1 µl of the PCR solution is pipetted onto the heater window and stirred gently with one of the SAW transducers on the long side of the chip, to dissolve the dried primers. After about 10 s the oil cover is applied. Before starting the PCR cycles, the epoxy silane array in the middle of the second heater is covered with same amount of doubly concentrated hybridization buffer and oil. Since the fluorescence of Cy3 is not excited by the blue light of the online detection unit, it can also be used for the hybridization experiments to check the amount of DNA in the droplet. After the DNA amplification the droplet is heated to 95 °C for denaturation and then moved acoustically to the second heater. The two droplets join together as soon as they touch

inside the oil. The heater is set to the hybridization temperature and the array is incubated for 45–60 min. For washing the array, the chip is taken out of the holder, stirred subsequently in 2 ×, 1 × and 0.5 × SSC buffer (150 mM NaCl, 15 mM sodium citrate pH 7, *Eppendorf*) and dried in a stream of N_2. The fluorescence of the DNA spots is scanned with a *GenePix* scanner.

3. Results

3.1 PCR cycle management

The chip-PCR chamber consists of a water droplet covered by an oil cap that is placed in the middle of the window in the heater structure (Fig. 3). The temperature is measured with the sensor line around the window while resistive heating is provided by the outer line. To investigate the temperature distribution on the chip, an IR image was taken at 95 °C. Fig. 4 shows the temperature distribution along a straight line beginning at the sensor and leading to the edge of the chip. When the sensor reads $T = 95$ °C the inner heater line is about 98 °C. The difference can be explained by the low heat conductivity of the $LiNbO_3$ (5.6 W mK^{-1}). To reach the sensor the heat has to bridge the 25 μm distance between the two lines through the bulk material. In the area around the heater the temperature drops fast. When an oil droplet is placed on the structure, covering the sensor, the temperature of the heater wire does not change significantly.

To yield more information about the temperature inside the water droplet covered by oil we used a thermochrome dye chromazone (*Eckart*) that changes its color from blue to white around 70 °C. The exact characteristic of the transition was measured with a diluted dye solution in a temperature controlled spectrometer. The transmission at 630 nm shows a typical sigmoid signal increase close to the transition temperature. We used this curve as a reference for the measurement inside the droplet. The transition on the chip was determined from the color change of the dye in a water droplet covered by oil. The observation was done with a video microscope. For the video, the temperature of the heater was raised in steps of 0.1 K s^{-1}. The colour values were determined

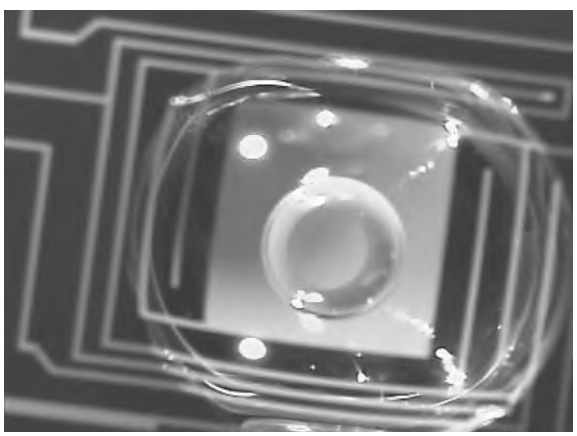

Fig. 3 Oil covered aqueous PCR solution in oil situated on a chip heater.

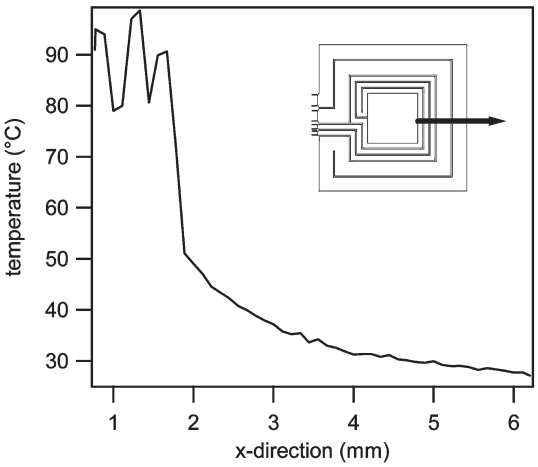

Fig. 4 Temperature distribution on the chip starting at the sensor of a thin film heater measured with an IR camera. The temperature was determined along the arrow shown in the insert. The heater was set to 95 °C. The inner heater wire reaches 98 °C, the outer 93 °C. For the measurement the chip was covered with gold outside the heater structures, since the camera is not able to measure on transparent substrates. In the gap between the heater and sensor the temperature can not be determined for the same reason. The different reflectivities of the platinum of the heater and the gold were taken into account for image processing.

from the images by video processing. The derivatives of the reference and the processed curve show a perfect match of the peaks marking the half point of the transition (Fig. 5). This means that the sensor temperature is the same as inside the PCR droplet. The varying widths of the transition peaks in Fig. 5 are caused by the methodical differences of the two techniques. Whereas in the spectroscopic method the transmission was measured at 630 nm, the image processing includes a wider colour range in the observation and therefore the transition appears broader.

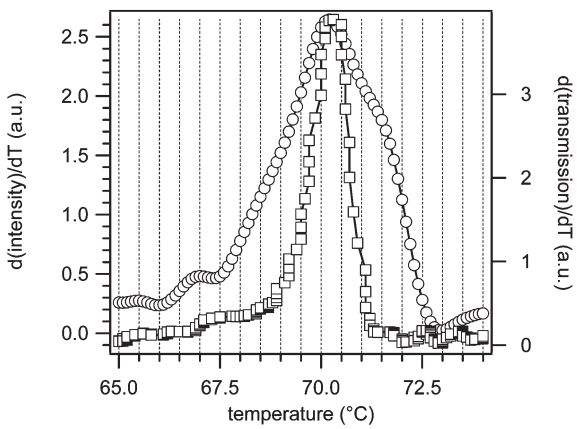

Fig. 5 Squares: The first derivative of the temperature dependent transmission of the chromazone dye measured with a temperature controlled spectrometer. The maximum, representing the half point of transition from blue to white, is at 70.3 °C. Circles: The first derivative of the color change from blue to white, measured with image processing on the chip heater. The maximum at 70.2 °C perfectly matches the spectrometer data.

Since the heat conductivity of the oil is 0.15 (W mK^{-1}) which is 37 times lower than that of the bulk material, the heat in the droplet is expected to be transported mainly by the $LiNbO_3$ and the oil serves as an insulation to the surrounding air. The video images of the dye experiments show a fast stirring of the solution during elevated temperatures, which should level gradients in the droplet.

The maximum heating rate on the chip is about 50 K s^{-1}, but for the PCR experiments best results are obtained at 10 K s^{-1}. The cooling rate at 25 °C ambient temperature is 5 K s^{-1}. Both heating and cooling rates are notedly higher than those of conventional thermal cyclers (1–2 K s^{-1}). This is because of the low thermal mass of the chip and the low heat capacity of the bulk material. A graph of three temperature cycles is shown in Fig. 6.

During the temperature cycles the chip was covered with a small plastic cap to avoid disturbing air streams. Inside the cap the loss of water by evaporation from the droplet after 35 PCR cyles was about 10%. The missing water had no influence on the efficiency of the PCR, it can also be avoided by putting a piece of wet wadding into the plastic cap.

3.2 PCR optimization

For the on-chip PCR three different surface modifications were tested. Best results were obtained with fluoroalkylsilanes that can also be structured by photolithography.

Before performing a PCR the chips have to be cleaned to remove all contaminations. Due to the high stability of the organic layer the chips can be cleaned with organic solvents and strong detergents without causing damages. The chips can be recycled for a number of PCRs. The efficiency of the cleaning procedure was tested by PCR without template. In these experiments no product appeared in the electrophoresis gels, showing that the cleaning is sufficient to remove all contaminations.

Two different metals were tested for the heater and sensor structure. Platinum is the common material used for thin film sensors, because of its strict linear resistance *vs.* temperature dependence (RTD). Nickel is much cheaper than Pt, but the RTD is slightly curved. To reach the same accuracy for the temperature measurement as Pt, an extra parameter is needed by the heater controller.

The water droplet inside the oil has a spherical shape with a flat region where it is in contact with the chip surface. This leads to a surface to volume ratio that is comparable or smaller than in conventional PCR tubes. Standard PCR kits therefore could be used without additional ingredients like BSA, detergents or PEG that prevent adsorption to the interfaces.

3.3 Sensitivity and specificity of the chip PCR

The effectivity of the PCR can be tested by reducing template concentrations until no product can be detected anymore after a large number of cycles. For the test, human genomic DNA was used with chromosome-specific primer pairs for the amplification of a 150 bp and a 1382 bp fragment. Genomic DNA can be considered a ''difficult'' template since it has a high sequential and spatial complexity. In a 1 µl droplet a successful amplification of the 1382 bp fragment could be completed in 35 cycles from as low as 6 genome equivalents (Fig. 7). Under the same conditions only one chromosome containing the 150 bp fragment was enough to produce a visible band on the electrophoresis gel (Fig. 8). This represents the maximum possible sensitivity that can be reached by a PCR device. This is even more remarkable when considering that the tests were done with genomic DNA. As stated in Fig. 8 the concentration used for the single template experiments is 0.1 genome equivalents. Following statistics, this means that the right template chromosome should be contained in every fifth PCR sample. From a series of experiments we determined that on the average two out of ten experiments are successful, which is in good accordance with statistics.

A well known problem of PCR is the lack of specificity for the desired product resulting in a number of longer or smaller fragments, that can also be detected after the process. To suppress the side products one has to optimize temperatures

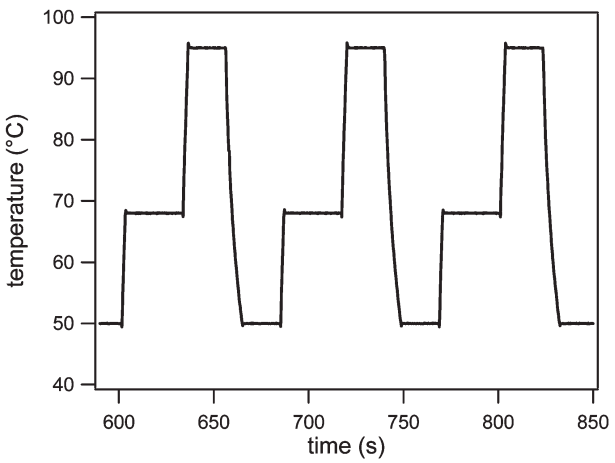

Fig. 6 Three temperature cycles performed with a chip heater with a heating rate of 10 K s^{-1} and a convective cooling rate of 5 K s^{-1}.

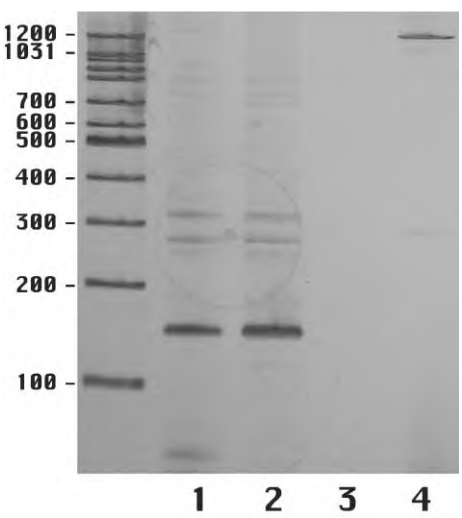

Fig. 7 Chip PCR (35 cycles) detected with electrophoresis gel. Lanes 1,2: 150 bp fragment of human genomic DNA cycled from 6000 genome equivalents (one genomic equivalent equals to 2 × 23 chromosomes); lane 3: no template; lane 4: 1382 bp fragment was amplified from 6 genome equivalents.

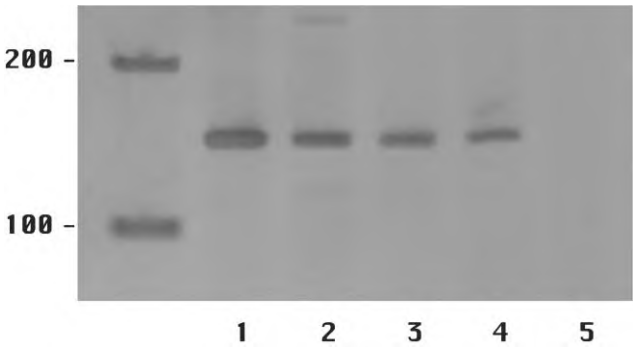

Fig. 8 Chip PCR (35 cycles) for the 150 bp fragment detected with electrophoresis gel with different template concentrations of human genome equivalents. Lanes 1: 120; 2: 12; 3: 1.2; 4: 0.1 (in accordance with statistics only every fifth PCR experiment was successful with this dilution containing approximately 4 chromosomes); 5: 0 genome equivalents.

and cycle times. We found that for the chip heater the accurate annealing time is crucial for a high selectivity. Depending on the primer/template system the window of annealing temperatures leading to successful amplification was 6–8 °C wide. The selectivity was highest at the upper end of the temperature interval. The chip heater generally showed a higher sensitivity than our commercially available tube cycler (*Mastercycler, Eppendorf*). The reason for that can probably be found in the fast heating and cooling rates (10 K s^{-1}, 5 K s^{-1}) and the small volume preventing temperature gradients.

3.4 Rapid operation and low volume

Another important aspect of miniaturized PCR devices besides the sensitivity and the specificity is the time needed for the amplification process. To test how short the cycle times can be chosen for the 150 bp fragment the cycle times were successively reduced. With a 5 s span for each of the three different temperatures one cycle can be completed within 20 s, which means a total time of 10 min for 30 cycles. For this period a successful amplification was demonstrated starting from 10 genomic equivalents. Depending on the desired concentration at the end and the amount of template molecules the process time could even be reduced further. Short process times also have a positive effect on the effectivity of the polymerase in the PCR solution, because the lifetime of the enzyme is reduced during the high temperature state.

Low volumes for the PCR improve the transport of heat during the PCR cycles and allow for the design of small devices. To check on this parameter, we reduced the normally used 1 µl for the PCR to lower volumes. The amount of 5 µl oil for the cover was kept constant. From a 200 nl droplet PCR with 200 templates a 150 bp band was still visible in the electrophoresis gel. Smaller volumes cannot be detected with the electrophoresis gel and were therefore not tested.

3.5 Online detection

A direct observation of the amount of DNA after each cycle can indicate if the amplification was successful and can help to optimize the PCR parameters. A large number of commercially available kits exists to detect the state of the PCR during the process using different kind of fluorescent dye systems. To explore the possibilities of online monitoring during the on-chip PCR, an optical unit for the detection of a fluorescence signal was assembled. The unit uses the principle of fluorescence microscopy with epi illumination of blue light at 490 nm. Both an image of the PCR droplet and the intensity of emitted light can be captured. The filters were chosen for the dye SYBR Green, that emits at 510 nm. The intensity of the emission depends on the amount of double stranded DNA (ds DNA) in the solution, because its quantum yield increases by orders of magnitude when it intercalates. At the end of every elongation phase the amount of ds DNA is the highest. At this point the intensity is captured by the software for every cycle. A reference signal is measured for every following denaturation. The ratio of the two signals is plotted to a graph in the software screen, so that the actual state of the PCR during the temperature cycles is continuously displayed. During a successful experiment the signal curves away from the plateau of the background at a certain cycle number and increases until a saturation is reached. The start point of the signal change depends on the template concentration.

To measure the sensitivity of the device, a series of PCRs with plasmid template numbers from 7×10^5–7×10^1 was performed on the same chip. Fig. 9 shows the intensity curves in question. The points where the signals rise from the plateau is plotted against the cycle number in Fig. 10. In a log plot the data can be fitted by a straight line. This can be expected for an ideal PCR where the amount of ds DNA is doubled for every cycle. A linear interpolation to the x-axis in Fig. 10 indicates a sensitivity limit of 10^8 copies or 0.1 ng of ds DNA.

Normally $V = 1$ µl solution was used for the online PCR droplet, but also smaller volumes were tested. For $V = 0.5$ µl the signal is still high enough to show a distinct result. Depending on the template concentrations also lower volumes

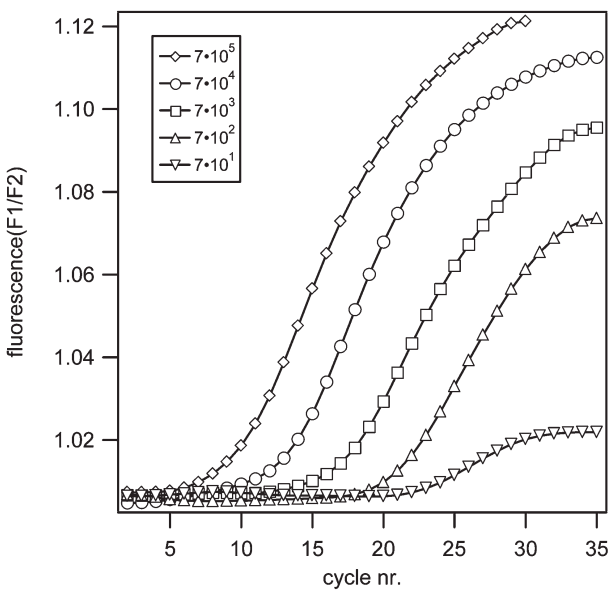

Fig. 9 Online PCR traces for 5 different template concentrations of plasmid. The point where the signal rises from the plateau at 1.0 is dependent on the concentration.

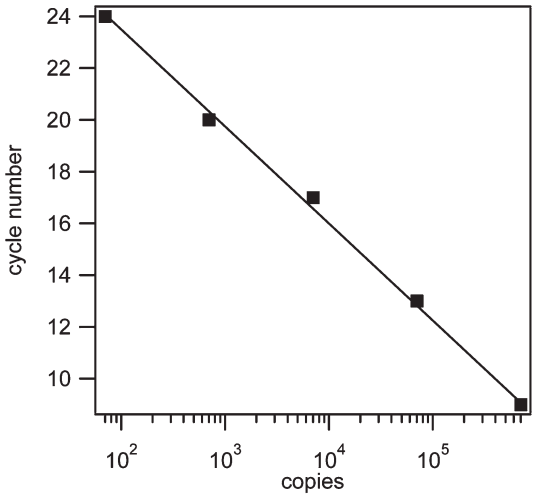

Fig. 10 The point where the signal in Fig. 9 rises from the plateau against the template concentration. The data can be fitted by a straight line. Interpolation of this line to the *x*-axis yields the sensitivity limit of the online detection.

than 0.5 µl are possible when the typical integration time of 1 s for the photodetector is increased. With 1 s integration time the shortest time for a complete cycle that can be handled by the software is 17 s. This means that each of the three temperatures is kept for 3 s. With the plasmid system the PCR was still successful for these short times (Fig. 11).

To test the reproducibility of the PCR curves 5 successive experiments were performed on the same chip. On the curves the start of the signal increase and the maximum of the first derivative appeared at the same cycle number. The maximum amplitude was dependent on the position of the droplet on the heater structure and therefore varies around 10–20%. This variation and the signal noise can be reduced when the surface

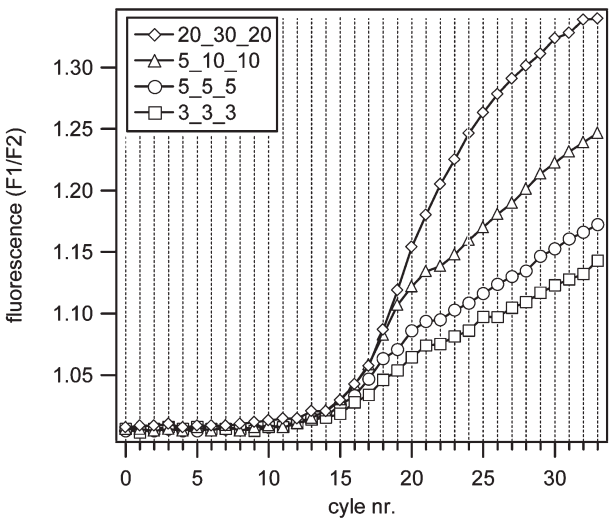

Fig. 11 A PCR (35 cycles, 700 templates) with the plasmid system can be performed in cycle times of 3 s for the three temperatures. The effectivity for these short times, however, is reduced compared to longer cycle times. The numbers in the graph annotation represent the time in seconds for: denaturation_elongation_annealing.

in the heater window is not a homogeneous hydrophobic surface, but is structured with a spot of PEG-silane. Owing to the hydrophilic character of this silane, the PCR droplet is anchored to the surface and the position is fixed. Since the contact area of the droplet with the surface is larger the signal intensity is increased as well.

When SYBR Green I is used for the online detection of the DNA amplification no specific information about the kind of ds-DNA in the solution is given. Commercial instruments like the *Lightcycler* (*Roche*) therefore use a melting curve analysis after the PCR cycles. This can help to identify the desired product, because the transition temperature from ss-DNA to ds-DNA depends on the length and sequence of the product. This feature was also included into the software. During a 0.1 K s^{-1} temperature increase the fluorescence signal can be recorded every second. As the main focus of the experiments lay on PCR followed by hybridization, that also can detect the desired product, the optical unit was designed for SYBR Green I only. This dye also has the advantage that the excitation is far away from that of Cy3 at the labeled primers.

3.6 Droplet movement

With the interdigitated transducers (IDT) on the $LiNbO_3$ substrate a SAW can be induced. With sufficient RF-power the wave can move a liquid droplet over the surface of the chip. In our preliminary experiments, fine tuning is done with a joystick connected to a multichannel RF-source. To keep the droplet in the acoustic path of the transducer two hydrophilic tracks were structured on the surface at the boundaries of the 3 mm wide path. This was done in the same process step that establishes the epoxysilane square in one of the heater windows. The four small transducers generating a SAW perpendicular to the large ones (see Fig. 2) cannot move the whole oil droplet, but allow for an exact alignment on the heater windows. They are also used for resolving dried primers into the PCR solution and to stir during hybridization.

For a PCR experiment with subsequent hybridization the epoxy array was covered with 1 µl double concentrated hybridization buffer and oil. After the temperature cycles the PCR droplet was pushed into the other. The two aqueous samples inside the oil merge as soon as they get in close contact, covering the spotted array with the correct buffer conditions. The unification works very reproducibly since the buffer on the hydrophilic array is fixed to its position and the moving droplet is kept on the right path with the fluidic tracks on both sides.

The aspect of contamination of the surface during the translation of the PCR products over the surface was investigated with a fluorescence test. After a high concentration of labeled DNA was moved, the remaining amount was monitored with a fluorescence scanner. No signal was detected on the surface for the moving DNA. Only when the droplet rested on the surface some molecules remained adsorbed.

3.7 Hybridization on chip

For a specific detection of the PCR product with hybridization on the integrated chip, an array of four oligonucleotide spots was printed into the epoxy square. Two test systems were

chosen for the experiments. The first was the plasmid with matching and totally mismatching oligos. More clinically relevant is the Factor V Leiden syndrome used as the second system. This disease is caused by a single nucleotide polymorphism (SNP) on the relevant gene and leads to increased blood coagulation. Oligos matching the product with and without the SNP were used for the array. Blood samples were taken from volunteers and purified with a commercial kit from *Quiagen*.

For the PCR with subsequent hybridization a small amount of the primer pair solution was dried on the window of the first heater. At the beginning of the experiments the primers were then dissolved into the PCR solution by gently mixing by SAW. With the online detection the state of the DNA amplification was observed. When the concentration of ds-DNA was high enough, the product was denaturated for 60 s and immediately transferred to the spotted array by SAW. The heater was set to the hybridization temperature for about 45–60 min. After cooling down, the oil was removed with a paper tissue and the chip was taken out of the holder and immersed in 2 × SSC, 1 × SSC and 0.5 × SSC. Finally the chip was dried in a stream of nitrogen and put to a fluorescence scanner. Two representative images for the plasmid and Factor V Leiden syndrome are shown in Fig. 12. For the latter the intensity difference between the spots is significantly smaller than with the plasmid, as can be expected for a SNP. Nevertheless a clear result can be obtained for both systems. When the solution was gently stirred during the hybridization the spots appeared more homogeneous and the fluorescence intensity was increased.

4. Discussion and outlook

We demonstrated a novel analytical microfluidic device based on the combination of a planar SAW chip with a chemically structured surface and miniaturized thin film resistant heaters. Instead of small channels the fluid is manipulated in oil covered droplets that can be ultrasonically actuated along the surface plane. We showed that with employing our device an analysis about the SNP causing the Leiden Factor V can be performed. The necessary primers for the template amplification and the probes for the hybridization can be applied to the chip surface and dried to create a single use assay for a special biological problem. The process steps that can be done on our device in the actual state are: Resolving the dried primers, placing the solution on the heater and covering it with oil. After running the PCR heating cycles the droplet can be moved to a second heater that generates the elevated temperature for the hybridisation on its surface. Micro devices that can perform PCR with subsequent hybridsation,[3,51–53] were designed by several groups, but to our knowledge, we present the first example of functional microfluidic device on a planar chip with a surface acoustic nanopump.

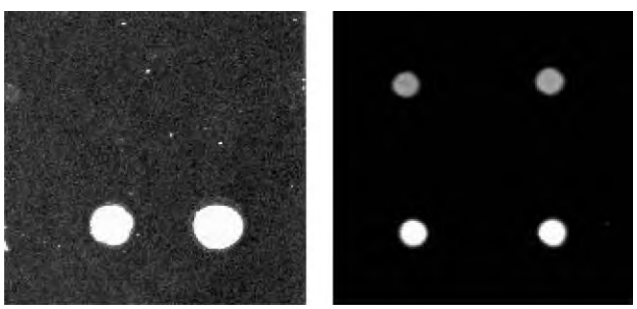

Fig. 12 Left: Hybridization on chip with the plasmid. The upper two spots are a total mismatch oligo. The lower two spots are a total match oligo. Right: Hybridization with the Leiden Factor V system. The oligos in the upper spots have one mismatch, the lower ones are a total match. The spot size is 90–110 μm.

A SAW chip has several advantages over microfluidic channel systems. Besides avoiding the problems of clogging, of large pressure drop and of large surface area, it enables one to resolve dried reaction components from the solid surface by actively mixing the fluid in a droplet. The stirring can also help to speed up a binding reaction and to get a more homogeneous fluorescence in hybridization. An oil cover forming a circular shaped cap on the hydrophobic surface reliably prevents evaporation. The PCR cycled in the oil cap, heated by the metal thin film structure has a unique performance as compared to both classical and microfluidic devices. It can reach the maximum sensitivity of only one template molecule of human genes with a high specificity. The sample volume can be as small as 200 nl, which is in the range of the smallest mentioned in literature. For one cycle the time can be reduced to 17 s due to the fast cycling rates and the effective heat distribution, which brings us close to the IR heated device of Giordano *et al.*[23] that completes 15 cycles in 4 min. The transparent $LiNbO_3$ also enables online monitoring to control the state of the DNA amplification. For detection purposes, we built a SYBR Green sensitive epi-fluorescence microscope with a sensitivity of 0.1 ng DNA. The modular design of the optical unit would allow for an extension with additional detection channels at wavelengths higher than 510 nm. They could be used for more specific dye systems than SYBR Green, using quenching or flourescence transfer effects.

The PCR oil compartment can be easily moved to the second heater and the change of buffer conditions for stringent hybridization is simply achieved by merging the PCR droplet with the liquid on the spotted array. Hybridization on the chip works reproducible with low background fluorescence. The experiments show that agitating with the SAW during the hybridization has an additional positive effect on the fluorescence intensity and the homogeneity of the spots. The specificity is high enough to clearly detect SNP with a tenfold difference in fluorescence intensity between the mutation and the wildtype.

After hybridisation, the whole chip was washed and the fluorescence of the DNA spots was scanned by a commercial scanner. Only a few attempts to integrate a hybridization array analysis are reported. One example is the electrochemical method.[52] It appears to be rather easy to integrate a small optical unit that can collect the emitted fluorescence light below the chip focussing through the transparent window in the hybridization heater. Due to the high refractive index of $LiNbO_3$ ($n = 2.2$) also evanescent illumination of the DNA spots could be used, which would allow for observation without washing.

Acknowledgements

This research was sponsored by VDIVDE, BMBF Mikrosystemtechnik 2000+ Projekt V2266 PCR-Chip, and in parts by the Bayrische Forschungsstiftung (FORNANO)

Zeno Guttenberg,*[a] Helena Müller,[a] Heiko Habermüller,[a] Andreas Geisbauer,[a] Jürgen Pipper,[b] Jana Felbel,[b] Mark Kielpinski,[b] Jürgen Scriba[a] and Achim Wixforth[ac]

[a]*Advalytix AG, Eugen-Sänger-Ring 4, 85649 Brunnthal, Germany. E-mail: guttenberg@advalytix.de*

[b]*Institut für Physikalische Hochtechnolgie e.V. Bereich Mikrosysteme, Albert-Einstein-Str. 9, 07745 Jena, Germany*

[c]*Lehrstuhl für Experimentalphysik I, Universität Augsburg, Universitätsstrasse 1, 81635 Augsburg, Germany*

References

1 E. Eteshola and D. Leckband, *Sens. Actuators B*, 2001, **72**, 129.
2 A. G. Hadd, J. M. Jacobson and J. M. Ramsey, *Anal. Chem.*, 1999, **71**, 5206.
3 D. J. Harrison, K. Fluri, K. Seiler, Z. Fan, C. S. Effenhauser and A. Manz, *Science*, 1993, **261**, 895–897.
4 J. Wang, M. P. Ibanez, A. Chatrahi and A. Escarpa, *Anal. Chem.*, 2001, **73**, 5323.
5 T. Thorsen, S. J. Maerkl and S. R. Quake, *Science*, 2002, **298**, 580–584.
6 A. Manz, C. S. Effenhauser, N. Burggraf, D. J. Harrison, K. Seiler and K. Fluri, *J. Micromech. Microeng.*, 1994, **4**, 257.
7 J. H. Wu and H. J. Keh, *Colloids Surf. A*, 2003, **212**, 27–42.
8 J. P. Brody, P. Yager, R. E. Goldstein and R. H. Austin, *Biophys. J.*, 1996, **71**, 3430–3441.
9 P. Wilding, M. A. Shoffner and L. J. Kricka, *Clin. Chem.*, 1994, **40**, 1815–1818.
10 L. J. Wilding, J. Kricka, G. Cheng and M. A. Hvichia, *Anal. Biochem.*, 1998, **257**, 95–100.
11 J. H. Daniel, S. Iqbal, R. B. Millington, D. F. Moore, C. R. Lowe, D. L. Leslie, M. A. Lee and M. j. Pearce, *Sens. Actuators A*, 1998, **71**, 81–88.
12 M. A. Northrup, B. Benett, D. Hadley, P. Landre, S. Lehew, J. Richards and P. Stratton, *Anal. Chem.*, 1998, **70**, 918–922.
13 M. Kopp, A. De Mello and A. Manz, *Science*, 1998, **280**, 1046–1048.
14 L. C. Waters, S. C. Jacobson, N. Kroutchinina, J. Khandurina, R. S. Foote and J. M. Ramsey, *Anal. Chem.*, 1998, **70**, 158–162.
15 R. P. Oda, M. A. Strausbusch, A. F. R. Huhmer, N. Borson, S. Jurrens, R. Craighead, J. Wetterstein, P. J. Wetterstein, B. Eckloff, B. Kline and J. P. Landers, *Anal. Chem.*, 1998, **70**, 4361–4368.
16 T. B. Taylor, S. E. Harvey, M. Albin, L. Lebak, Y. Ning, I. Mowat, T. Schuerlein and E. Principe, *Biomed. Microdev.*, 1998, **1**, 65–70.
17 L. Kricka, P. Fortina, N. Panaro, P. Wilding, G. Alonso-Amigo and H. Becker, *Lab Chip*, 2002, **2**, 1–4.
18 P. Grodzinski, R. H. Liu, D. Rhine, D. Weston, D. Ganser, C. Romero, A. Schneider, J. Blackwell, H. Chen, Y. Liu and T. Smekal, *Biomed. Microdev.*, 2001, **3**, 275.
19 J. B. Findlay, S. Atwood, M. I. Bergmeyer, J. Chemelli, K. Christy, T. Cummins, W. Donish, T. Ekeze, J. Falvo and D. A. O. Patterson, *Clin. Chem.*, 1993, **39**, 1927–1933.
20 I. Schneegaß, R. Bräutigam and J. M. Köhler, *Lab Chip*, 2001, **1**, 42–49.
21 J. Khandurina, T. E. Mcknight, S. C. Jacobson, L. C. Waters, R. S. Foote and J. M. Ramsey, *Anal. Chem.*, 2000, **72**, 2995–3000.
22 H. Nagai, Y. Murakami, Y. Morita, K. Yokoyama and E. Tamiya, *Anal. Chem.*, 2001, **73**, 1043–1047.
23 B. C. Giordano, J. Ferrance and S. Swedberg, *Anal. Biochem.*, 2001, **291**, 124–132.
24 E. T. Lagally, I. Medintz and R. A. Mathies, *Anal. Chem.*, 2001, **73**, 565–570.
25 E. T. Lagally, P. C. Simpson and R. A. Mathies, *Sens. Actuators B*, 2000, **63**, 138–146.
26 J. B. Brzoska, A. I. Ben and F. Rondelez, *Langmuir*, 1994, **10**, 4367–4373.
27 A. Ulman, *Chem. Rev.*, 1996, **96**, 1533–1554.
28 S. Frank, *Prog. Surf. Sci.*, 2000, **65**, 151–256.
29 Y. Xia and G. M. Whitesides, *Angew. Chem. Int. Ed.*, 1998, **37**, 550–575.
30 M. G. Pollack and R. B. Fair, *Appl. Phys. Lett.*, 2000, **77**, 1725–1728.
31 J. S. Kuo, P. Spicar-Mihalic, I. Rodriguez and D. T. Ciu, *Langmuir*, 2003, **19**, 250–255.
32 S. K. Cho, H. Moon and C.-J. Kim, *J. Microelectromech. Syst.*, 2003, **12**, 70–80.
33 B. Liedberg and P. Tengvall, *Langmuir*, 1995, **11**, 3821–3827.
34 S. Welin-Klintström, M. Lestelius, B. Liedberg and P. Tengvall, *Colloids Surf. B*, 1999, **15**, 81.
35 K. Ichimura, S. K. Oh and M. Nakagawa, *Science*, 2000, **288**, 1624.
36 D. F. Dos Santos and T. Odarcuhu, *Phys. Rev. Lett.*, 1995, **75**, 2972–2975.
37 I. F. Lyuksyutov, D. G. Naugle and K. D. D. Rathnayaka, *Appl. Phys. Lett.*, 2004, **85**, 1817–1819.
38 S. Shiokawa, Y. Matsui and T. Ueda, *IEEE Ultrason. Symp.*, 1989, 643–646.
39 T. Uchida, T. Suzuki and S. Shiokawa, *IEEE Ultrason. Symp.*, 1995, 1081–1084.
40 Z. Guttenberg, A. Rathgeber, S. Keller, J. O. Rädler, A. Wixforth, M. Kostur, M. Schindler and P. Talkner, *Phys. Rev. E*, 2004, **70**, 056311.
41 C. J. Strobl, Z. Guttenberg and A. Wixforth, *IEEE Trans. Ultrason., Ferroelectrics, Frequency, Control*, 2004, **51**, 1432.
42 K. B. Mullis, F. Ferre and R. A. Gibbs, *The Polymerase Chain Reaction*, 1994, Birkhauser, Boston.
43 M. Schena, *DNA Microarrays: a Practical Approach*, 1999, Oxford University Press, Oxford, Hong Kong.
44 S. Dong, E. Wang, L. Hsie, Y. Cao, X. Chen and T. R. Gingeras, *Genome Res.*, 2001, **11**, 1418–1424.
45 M. O. Noordewier and P. V. Warren, *Trends Biotechnol.*, 2001, **19**, 412–415.
46 C. T. Wittner, K. M. Ririe, R. V. Andrew, D. A. David, R. A. Gundry and U. J. Balis, *BioTechniques*, 1997, **22**, 176–181.
47 P. Belgrader, S. Young, Y. Bob, M. Primeau, L. A. Christel, F. Pourahmadi and M. A. Northrup, *Anal. Chem.*, 2001, **73**, 286–289.
48 C. T. Wittner, G. Mark, H. A. A. Moss and R. P. Rasmussen, *BioTechniques*, 1997, **22**, 130–137.
49 P. Belgrader, W. Benett, D. Hadley, J. Richards, P. Stratton, J. Mariella and F. Milanovich, *Science*, 1999, **284**, 449–450.
50 W. L. Nyborg, *Acoustic Streaming*, in *Nonlinear Acoustics*, 1998, Academic Press, San Diego.
51 Y. Liu, C. B. Rauch, R. L. Stevens, R. Lenigk, J. Yang, D. B. Rhine and P. Grodzinski, *Anal. Chem.*, 2002, **74**, 3063–3070.
52 T. Ming Hung Lee, M. C. Carles and I.-M. Hsing, *Lab Chip*, 2003, **3**, 100–105.
53 R. C. Anderson, X. Su, G. J. Bogdan and J. Fenton, *Nucl. Acids Res.*, 2000, **28**, E60.